CONF-9505264--34

UCRL-JC-118105
PREPRINT

Design and Performance of the Beamlet Laser Third Harmonic Frequency Converter

C. E. Barker, B. M. Van Wonterghem, J. M. Auerbach,
R. J. Foley, J. R. Murray, J. H. Campbell,
J. A. Caird, D. R. Speck, and B. Woods

This paper was prepared for submittal to the
1st Annual International Conference on Solid-State
Lasers for Application to Inertial Confinement Fusion
Monterey, CA
May 30-June 2, 1995

September 12, 1995

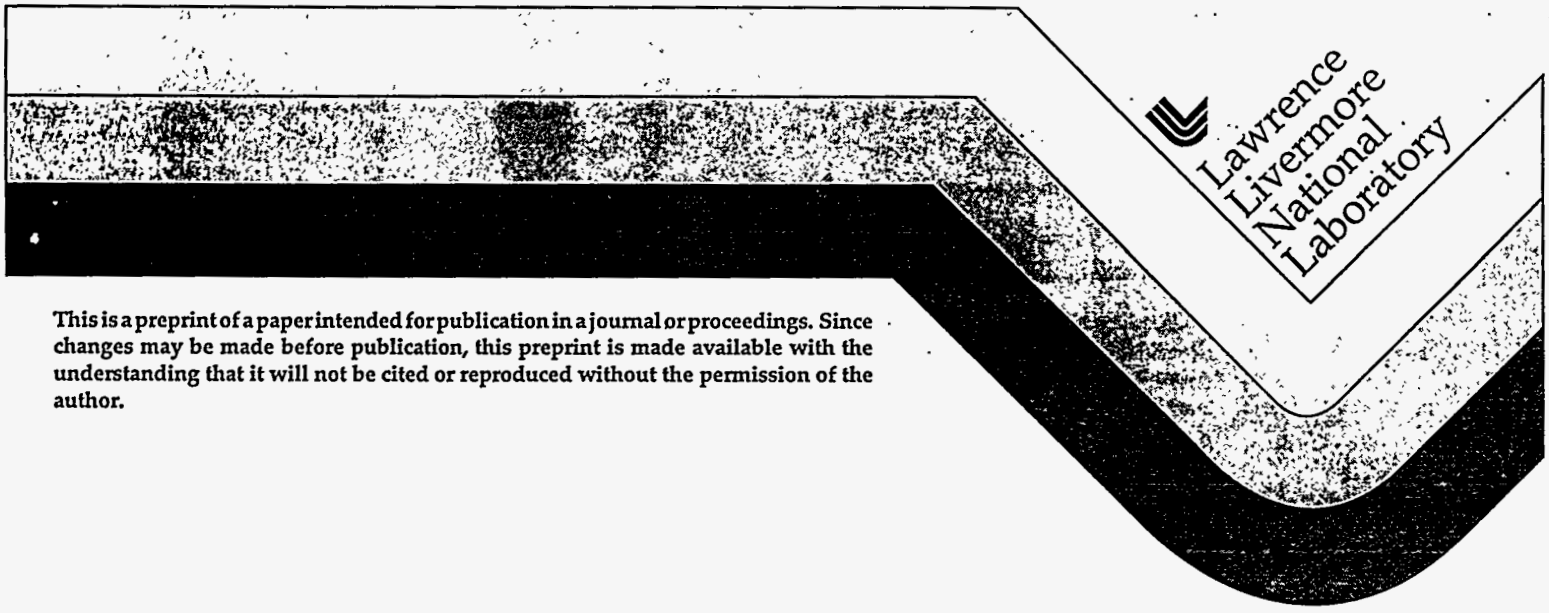

DLC

DISCLAIMER

Design and performance of the Beamlet laser third harmonic frequency converter

C. E. Barker, B. M. Van Wonterghem, J. M. Auerbach, R. J. Foley,
J. R. Murray, J. H. Campbell, J. A. Caird, D. R. Speck, and B. Woods

University of California
Lawrence Livermore National Laboratory
P. O. Box 5508, L-490
Livermore, CA 94551-9900, USA
(510) 423-3282 / FAX (510) 422-7748

ABSTRACT

The Beamlet laser is a full-scale, single-aperture scientific prototype of the frequency-tripled Nd:glass laser for the proposed National Ignition Facility. At aperture sizes of 30 cm × 30 cm and 34 cm × 34 cm using potassium dihydrogen phosphate crystals of 32 cm × 32 cm and 37 cm × 37 cm, respectively, we have obtained up to 8.3 kJ of third harmonic energy at 70% - 80% whole beam conversion efficiency.

Keywords: harmonic generation, frequency conversion, nonlinear optics

1. INTRODUCTION

The Beamlet Demonstration Project laser is a full scale, single-aperture scientific prototype of the frequency-tripled Nd:glass laser driver for the proposed National Ignition Facility (NIF). In contrast to the Nova laser, in which each beamline's third harmonic generator consists of two cascaded nonlinear optical crystal arrays each of which is tiled with nine 27 cm potassium dihydrogen phosphate (KDP) crystals,[1] the Beamlet laser's frequency converter uses a single sequential pair of 32 cm or 37 cm KDP crystals to generate light at the third harmonic. Whereas a Nova harmonic generation array routinely produces up to 4.5 kJ of third harmonic light at a conversion efficiency of about 55% (with a few experiments reaching 8 kJ of third harmonic at an efficiency of 70%),[1] Beamlet has demonstrated sustained *whole beam* third harmonic conversion efficiencies of 70-80%, producing up to 8.3 kJ of third harmonic light in a 3 ns pulse.

2. THIRD HARMONIC CONVERTER DESIGN

Third harmonic generation for Beamlet is accomplished by a sequential application of collinear sum-frequency mixing in two nonlinear optical crystals. A beam at the fundamental laser frequency enters the first crystal (the "doubling" crystal) in which a large fraction of the incident light is converted to the second harmonic frequency via degenerate sum-frequency mixing. The copropagating second harmonic and residual fundamental beams that emerge from the doubling crystal enter the second crystal (the "tripling" crystal) where a third harmonic beam is created by sum-frequency mixing of the fundamental and second harmonic beams.

The efficiency with which energy is transferred from the fundamental wave to the harmonic waves is dependent upon a number of parameters, of which phase-mismatch and photon flux balance ("mix ratio") are particularly important. Phase-mismatch is the difference between the k-vector of the output wave and the sum of the k-vectors of the input waves. Maximum energy transfer from the input waves to the generated waves occurs when the phase-mismatch is zero. This condition is usually achieved in nonlinear optical crystals by using the birefringence of the crystal to balance the effects of normal dispersion. This leads rather naturally to two types of phase matching: type I in which the input waves have the same polarization inside the crystal, and type II in which the two input waves are orthogonally polarized.[2]

Third harmonic generation efficiency is extremely sensitive to the ratio of the fundamental and second harmonic photon fluxes (mix ratio) entering the tripling crystal.[3] Craxton[3] has proposed two methods for controlling the mix ratio by adjusting the second harmonic generation efficiency in the doubling crystal: (1) adjusting the phase-mismatch of the second harmonic generation pro-

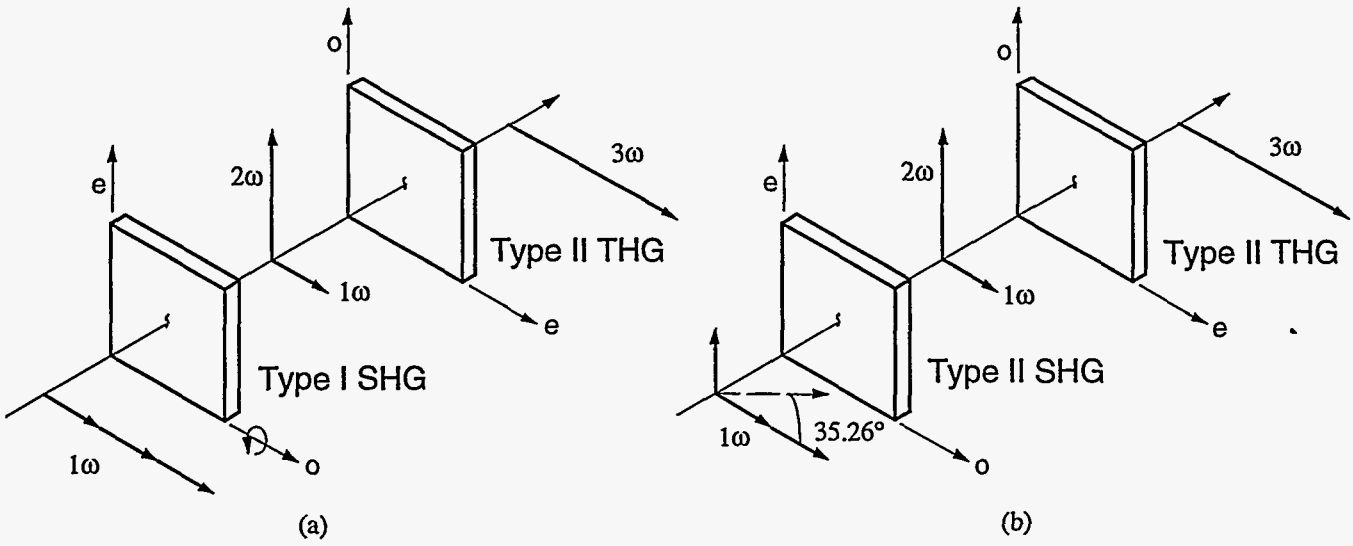

Figure 1. Cascaded type I / type II (a) and type II / type II (b) third harmonic generation schemes. In the type I / type II scheme mix ratio is controlled by angularly detuning the doubling crystal from perfect phase-matching. In the type II / type II scheme, mix ratio is controlled by the input polarization direction relative to the crystal axes. This is most conveniently accomplished by rotating the crystals about the beam propagation direction.

cess by angularly detuning the doubling crystal from perfect phase-matching; or (2) adjusting the polarization of the fundamental wave incident on the doubling crystal. With two types of phase-matching and two methods of mix ratio control, there are eight possible configurations for the third harmonic generator. For Beamlet and NIF we have considered the following two third harmonic generator designs: 1) type I second harmonic generation followed by type II third harmonic generation with the mix ratio controlled by angular detuning of the doubling crystal from perfect phase-matching; and 2) type II second harmonic generation followed by type II third harmonic generation for which the mix ratio is controlled by adjusting the polarization of the incident fundamental beam relative to the doubling crystal axes. These two schemes are depicted schematically in Figure 1. The remaining six configurations can be rejected on the basis of large sensitivities to a particular parameter or the need for special waveplates.

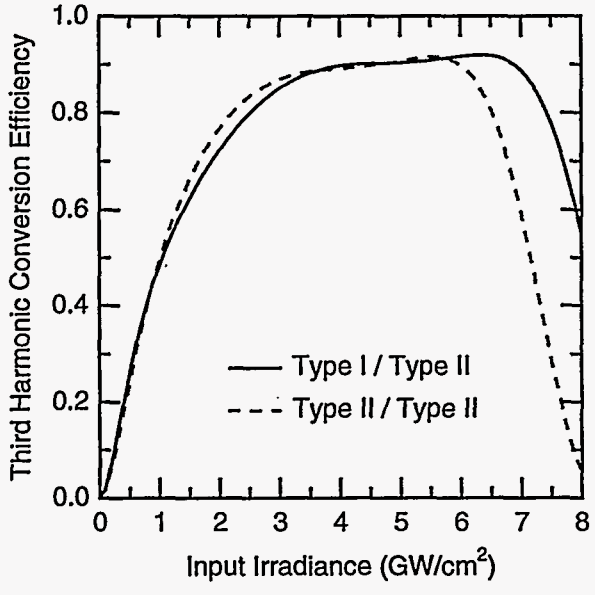

Figure 2. Third harmonic conversion efficiency versus input irradiance. The type I /type II design uses a 10.5 mm thick doubler detuned by 250 μrad. The type II / type II design uses an 8 mm thick doubler. Both designs use 9 mm thick triplers.

The type I / type II and the type II / type II designs were compared on the bases of dynamic range, angular sensitivity, and polarization sensitivity. As demonstrated by the plot in Figure 2, both designs offer similar dynamic range. The type I / type II design is more angularly sensitive than the type II / type II design, as the graph in Figure 3 indicates. However, the focusability requirements of both Beamlet and the NIF place tighter requirements on beam quality than that which is necessary for good efficiency from the type I / type II design. The type II / type II design is very sensitive to depolarization of the fundamental beam entering the doubler, as shown by the plot in Figure 4. As little as 0.5% of the input energy residing in the wrong polarization poisons the conversion process and tremendously reduces the third harmonic conversion efficiency. To obtain high conversion efficiency from the type II / type II design in the presence of even small amounts

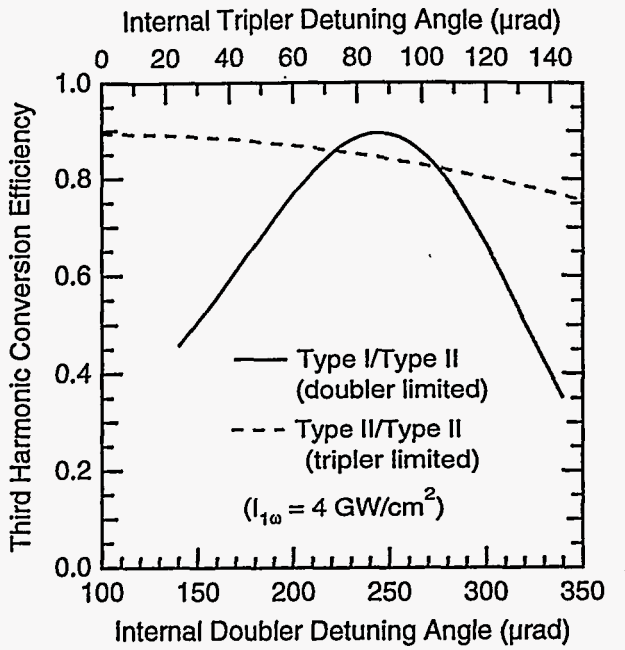

Figure 3. Third harmonic conversion efficiency versus crystal angles for the thicknesses listed in Fig. 2 and an input irradiance of 4 GW/cm². The sensitivity of the type I/type II design is dominated by doubler detuning (bottom scale). The sensitivity of the type II/type II design is dominated by the tripler detuning (top scale).

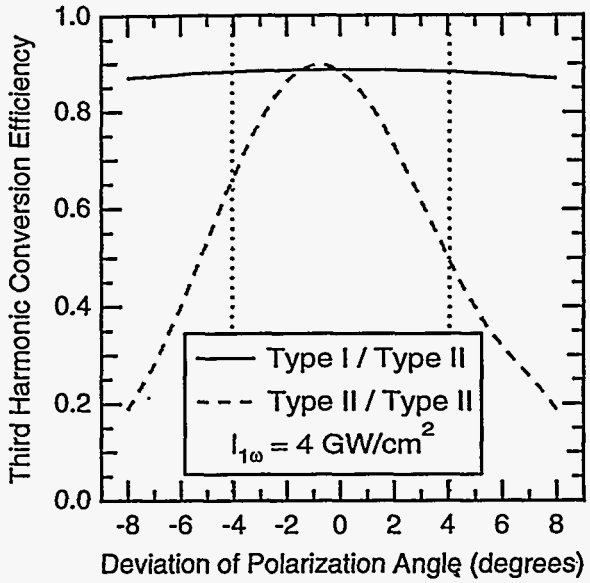

Figure 4. Third harmonic conversion efficiency versus input polarization error. The vertical dashed lines at ±4° correspond to a beam with 0.5% of its energy carried in the "wrong" polarization. The curves were calculated for an input irradiance of 4 GW/cm² and the crystal thicknesses given in Fig. 2.

of depolarization, the fundamental beam should be repolarized before it enters the doubling crystal. Such polarizers, however, would need to withstand very high beam fluences.

Another consideration in the selection of a third harmonic converter design for large aperture lasers is the size of the crystal boule required to produce the correctly oriented plates for a particular design. The orientations of the plates required for the type I / type II and type II / type II designs are shown in Figure 5. The minimal boule sizes necessary to produce 37 cm × 37 cm plates are given in Table 1. The increased size of the boule required to produce type II / type II plates is due to the additional rotation about face normal which is necessary to accommodate a square beam while simultaneously achieving the desired input polarization state without using a waveplate.

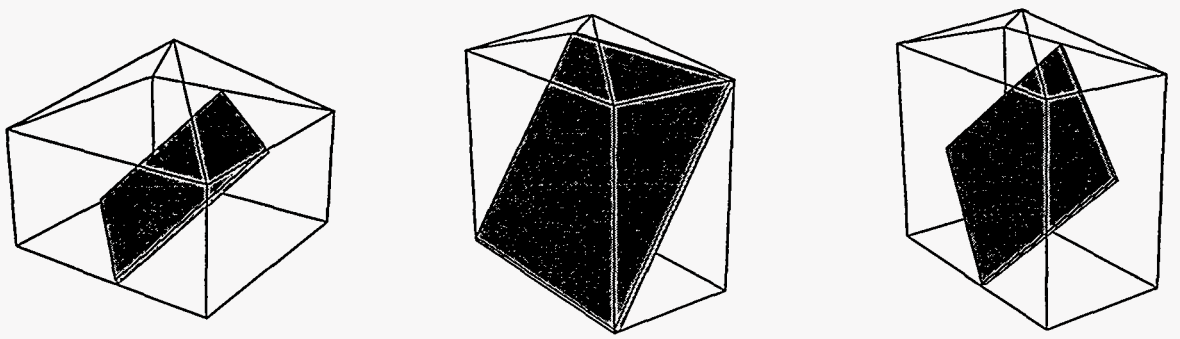

Figure 5. Oriented harmonic generation crystal plates within minimally-sized KDP crystal boules.

Table 1. Minimum crystal boule size requirements for 37 cm × 37 cm oriented plate

plate orientation (phase-matching type)	x dimension (cm)	y dimension (cm)	z dimension (cm) (parallel to c-axis)
type I SHG	46.4	46.4	25.0
type II THG (type I / II)	20.5	37.0	31.9
type II SHG/THG (type II / II)	28.2	51.6	44.6

We have chosen the type I / type II design as the baseline harmonic generator for Beamlet and for NIF. This selection was made on the bases of angular and polarization sensitivities, and the sizes of the crystal boules needed to produce frequency converter plates of the appropriate size. The type I / type II design is quite insensitive to depolarization and we lack the high-damage-threshold polarizers that are needed to obtain high conversion efficiency with the type II / type II design in the presence of small amounts of depolarization. The angular sensitivity of the type I / type II design is of secondary importance because the focusability specifications of the laser beam require beam quality that is sufficient for very good performance from the type I / type II design. The smaller crystal boules needed for the type I / type II design take less time to grow. Consequently the type I / type II design has lower risk with respect to obtaining the necessary crystal plates. The largest KDP and KD*P boules grown for Beamlet weighed nearly 800 lbs and took two years to grow.

The doubling crystal was cut from a single-crystal boule of KDP and finished by single-point diamond turning. The tripler was fabricated from 80% deuterated KDP to reduce the threat of damage from transverse stimulated Raman scattering.[4] Both faces of both crystals are SiO_2 sol-gel AR coated. The input and output faces of the doubler and the input face of the tripler are coated for maximum transmission at a wavelength of 700 nm, which provides very high transmission at both 1054 nm and 527 nm while simplifying the coating process. The exit face of the tripler is coated for maximum transmission at 351 nm.

Each of the two frequency conversion crystals is held by its corners in a diamond-turned mounting ring that is attached to a large optical mount that provides microradian-precision tilt about horizontal and vertical axes, as well as rotation about the beam propagation direction. Each mount can also be translated into and out of the beam path independently. This mounting system is designed to hold either 32 cm or 37 cm crystals. The layout of the third-harmonic frequency converter is shown in Figure 6, along with the output diagnostic beamsplitter and diagnostic focusing lens that are used to deliver a sample of the output beam to the

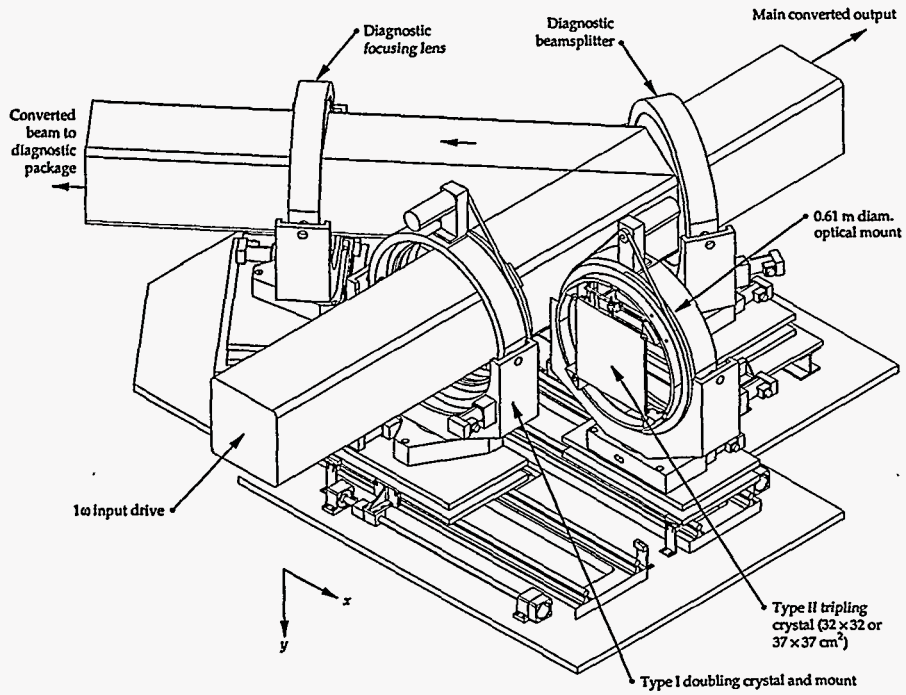

Figure 6. Layout of the third harmonic generator. Each crystal is carried in an independent optical mount. Enclosed within the same housing as the converter crystal assemblies are the output diagnostic beamsplitter and the diagnostic focus lens.

output diagnostic package.[5] The frequency conversion crystals and these two diagnostic optics are enclosed by an insulated housing within which temperature is controlled to ±0.05 °C, relative humidity is held to less than 35%, and cleanliness is maintained to better than class 10.

3. THIRD HARMONIC PERFORMANCE

The Beamlet harmonic generation system was activated initially with 32 cm square crystals that support a square beam aperture of 30 cm with an 84% fill factor. The third harmonic generator was activated in two stages. After installation of the doubler, its phase-matching direction was located initially by a series of low-power front end shots that were used to map out the second harmonic generation rocking curve. We then used high-power, 1 ns pulse-duration system shots to characterize the doubler performance at high irradiance and fine-tune its alignment. The plot in Figure 7 shows second harmonic conversion efficiency versus input irradiance for this series of shots; the maximum second harmonic conversion efficiency we measured was 83% at an input drive of 5.1 GW/cm^2. During this shot series the doubler was intentionally detuned by ±250 μrad and ±350 μrad to verify the phase-matching direction in the crystal. The solid curves shown in the figure were generated by a simple, idealized plane-wave model.

Upon completion of the doubler performance measurements, we installed the tripling crystal and located its phase-matching direction approximately with a series of low-power front-end shots. We then slowly increased the incident fluence on the crystal in order to damage-condition it. We also angularly tuned both crystals with high-power 1 ns pulses to optimize third harmonic conversion efficiency. The plot in Figure 8 shows third harmonic generation efficiency data versus input irradiance at 1054 nm for 3 ns duration pulses. The conversion efficiencies shown in the plot are simply whole beam energy ratios, i.e. total energy out at the third harmonic divided by total energy input at the fundamental. We observed a maximum third harmonic conversion efficiency of

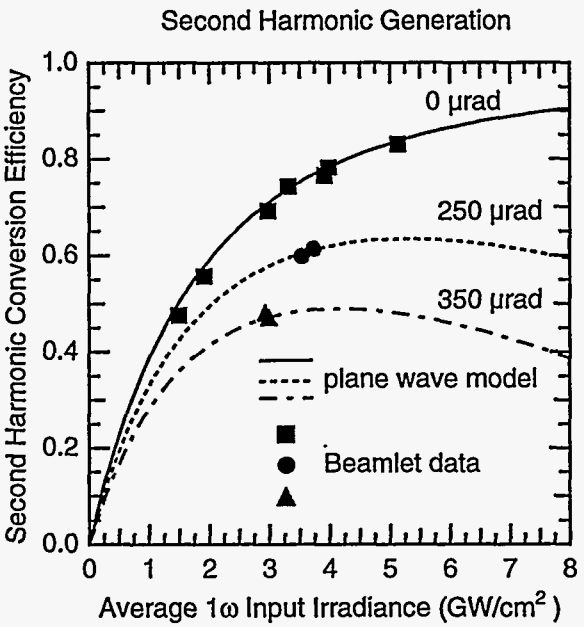

Figure 7. Second harmonic conversion efficiency versus average input irradiance using a 32 × 32 × 1.05 cm type I KDP doubler. The Beamlet data were generated with 1 ns square pulses in a 29.6 × 29.6 cm aperture with an 84% fill factor. Maximum second harmonic generation efficiency observed was 83% at an input irradiance of 5.1 GW/cm^2. The continuous curves were generated with a plane wave model.

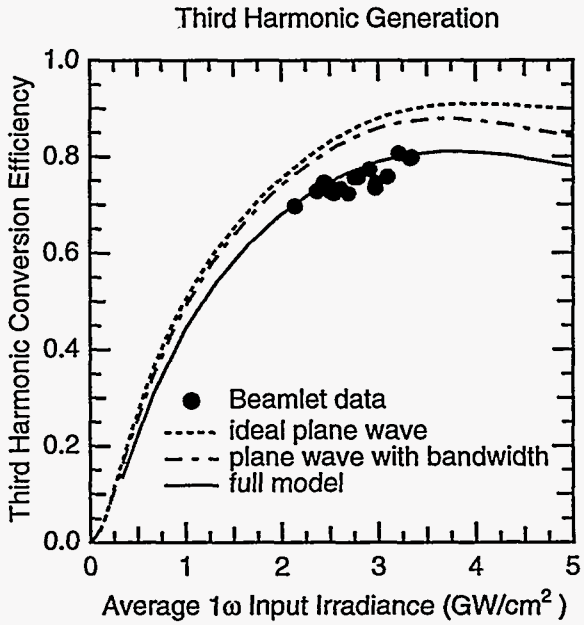

Figure 8. Third harmonic conversion efficiency versus average input irradiance using 32 cm square KDP crystals. The type I doubler was 1.05 cm thick and the type II 80% deuterated tripler was 0.95 cm thick. The Beamlet data was generated with 3 ns square pulses in a 29.6 × 29.6 cm aperture with an 84% fill factor. Maximum efficiency was 80.6% at an input irradiance of 3.3 GW/cm^2; maximum energy was 6.4 kJ.

80.6% at an input drive of 3.3 GW/cm^2. The maximum third harmonic energy produced at this 30 cm aperture size was 6.4 kJ, which provided an average third harmonic fluence of 8.7 J/cm^2. The solid curves shown in Figure 8 are calculated from an ideal plane wave model, which represents the maximum possible conversion efficiency, a plane wave model with phase-modulated bandwidth, and our current full model of the converter performance. This full model incorporates the effects of phase-modulated bandwidth, spatial and temporal pulse shape and modulation, and the non-flat character of the conversion crystals.

Our next set of harmonic generation experiments was performed with 37 cm converter crystals and a 34 cm beam aperture at an 88% fill factor. As we did with the 32 cm crystals, we activated the doubler first, following the same procedure of aligning the crystal with front-end shots followed by fine-tuning and performance verification with high power 1 ns system shots. The plot in Figure 9 shows the measured second harmonic conversion efficiency versus input irradiance from this set of laser shots. We then installed and aligned the tripler, again using rod shots to locate the phase-matching direction in the crystal. High power shots at 1 ns pulse duration were used to fine tune the alignment of both crystals. As indicated in the plot in Figure 10, system shots of increasing energy were then carried out at 1.7 ns and 3 ns pulse lengths, culminating in an output energy of 8.3 kJ of third harmonic at an average fluence of 8.2 J/cm^2. The maximum third harmonic conversion efficiency observed during these shots was 72%. At least part of the reduction in conversion efficiency from that observed during the 32 cm crystal experiments appears to be attributable to crystal mounts that warp the larger crystals. Future frequency converter designs will address this issue.

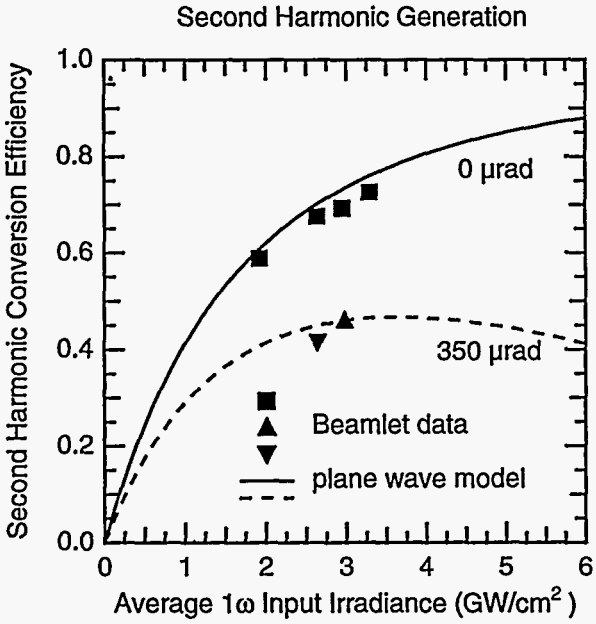

Figure 9. Second harmonic conversion efficiency versus average input irradiance using a 37 × 37 × 1.05 cm type I KDP doubler. The Beamlet data were generated with 1 ns square pulses in a 34 × 34 cm aperture with an 88% fill factor.

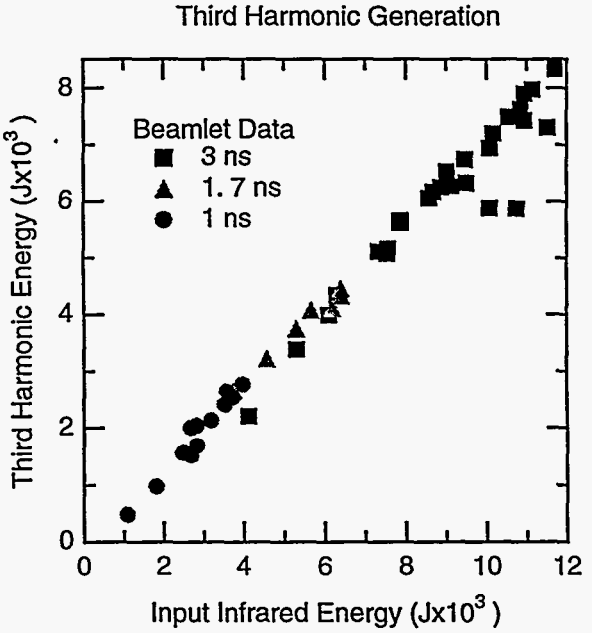

Figure 10. Third harmonic pulse energy versus input pulse energy using 37 cm KDP crystals; the type I doubler was 1.05 cm thick, and the 80% deuterated type II tripler was 9.5 cm thick. The Beamlet data were generated with 1 ns, 1.7 ns, and 3 ns square pulses in a 34 × 34 cm aperture with an 88% fill factor. The maximum third harmonic energy generated was 8.3 kJ.

4. ACKNOWLEDGEMENTS

We acknowledge the LLNL engineers, technicians, scientists, and support personnel whose efforts made Beamlet possible. We also acknowledge the many vendors whose high quality, state-of-the-art components were used in building the Beamlet laser. This work was performed under the auspices of the U. S. Department of Energy by Lawrence Livermore National Laboratory under contract No. W-7405-ENG-48.

5. REFERENCES

1. P. J. Wegner, M. A. Henesian, D. R. Speck, C. Bibeau, R. B. Ehrlich, C. W. Laumann, J. K. Lawson, and T. L. Weiland, "Harmonic conversion of large-aperture 1.05-μm laser beams for inertial-confinement fusion research," *Appl. Opt.*, Vol. 31, No. 30, pp. 6414-6426, Oct. 1992.

2. J. E. Midwinter and J. Warner, "The effects of phase matching method and of uniaxial crystal symmetry on the polar distribution of second-order non-linear optical polarization," *Brit. J. Appl. Phys.*, Vol. 16, pp. 1135-1142, 1965.

3. R. S. Craxton, "High Efficiency Frequency Tripling Schemes for High-Power Nd:Glass Lasers," *IEEE J. Quantum Electron.*, QE-17, No. 9, pp. 1771-1782, Sept. 1981.

4. J. H. Campbell, L. J. Atherton, J. J. DeYoreo, M. R. Kozlowski, R. T. Maney, R. C. Montesanti, L. M. Sheehan, C. E. Barker, "Large-Aperture, High-Damage-Threshold Optics for Beamlet," *ICF Quarterly Report*, Vol. 5, No. 1, pp. 68 - 79, Lawrence Livermore National Laboratory, Livermore, CA, UCRL-LR-105821-95-1, Oct. - Dec. 1994.

5. S. C. Burkhart, W. C. Behrendt, and I. Smith, "Beamlet Laser Diagnostics," *ICF Quarterly Report*, Vol. 5, No. 1, pp. 68 - 79, Lawrence Livermore National Laboratory, Livermore, CA, UCRL-LR-105821-95-1, Oct. - Dec. 1994.